Electrochemistry Communications 129 (2021) 107077

Contents lists available at ScienceDirect

Electrochemistry Communications

journal homepage: www.elsevier.com/locate/elecom

Layered transition metal selenophosphites for visible light photoelectrochemical production of hydrogen

Michela Sanna [a], Siowwoon Ng [a], Martin Pumera [a,b,c,d,*]

[a] Future Energy and Innovation Laboratory, Central European Institute of Technology, Brno University of Technology, Purkyňova 123, 61200 Brno, Czech Republic
[b] 3D Printing & Innovation Hub, Department of Food Technology, Mendel University in Brno, Zemedelska 1, 61300 Brno, Czech Republic
[c] Department of Chemical and Biomolecular Engineering, Yonsei University, 50 Yonsei-ro, Seodaemun-gu, Seoul 03722, Republic of Korea
[d] Department of Medical Research, China Medical University Hospital, China Medical University, No. 91 Hsueh-Shih Road, Taichung 40402, Taiwan

ARTICLE INFO

Keywords:
2D materials
Transition metal selenophosphites
Photoelectrocatalyst
Hydrogen evolution reaction
Photoelectrochemistry

ABSTRACT

The growing consumption of global energy has posed serious challenges to environmental protection and energy supplies. A promising solution is via introducing clean and sustainable energy sources, including photoelectrochemical hydrogen fuel production. 2D materials, such as transition metal trichalcogenphosphites ($MPCh_3$), are gaining more and more interest for their potential as photocatalysts. Crystals of transition metal selenophosphites, namely $MnPSe_3$, $FePSe_3$ and $ZnPSe_3$, were tested as photocatalysts for the hydrogen evolution reaction (HER). $ZnPSe_3$ is the one that exhibited the lowest overpotential and the higher response to the light during photocurrent experiments in acidic media. For this reason, among the crystals in this work, it is the most promising for the photocatalyzed production of hydrogen.

1. Introduction

The generation of carbon free fuels, such as hydrogen from water, is at the forefront of research to reduce the emission of harmful compounds in the atmosphere. The water splitting to hydrogen can be carried out directly via solar light energy [1], however, the yields of direct photochemical water splitting are low [2–4]. Alternatively, the solar energy is converted to electricity via solar panels and electrical energy to be used for water splitting via electrocatalysts, such as Pt or transition metal dichalcogenides [5–8]. The combination of both approaches, photoelectrochemical water splitting, combines the best from both worlds – electrocatalytical water splitting with the aid of photons [9–11].

Since 2004, when a simple procedure to obtain single-layer graphene was proposed by Novoselov et al. [12], a renewed interest in two-dimensional (2D) materials has grown rapidly. The scientific community started to focus on the study of the remarkable properties and the possible applications of these materials, starting with mono-element compounds, like graphene, and then moving to more complex ones, for example transition metal dichalcogenides [6,7,13]. The common feature in 2D materials is their peculiar structure: in their bulk form they present stacked layers, one on top of each other. The in-plane bonds are strong, however, the interactions between the layers are weaker, and this allows obtaining single or few layers by exfoliation or delamination [14–17].

Among the rediscovered 2D materials, transition-metal trichalcogenphosphites ($MPCh_3$) are gaining more and more interest in particular due to their catalytic properties in the hydrogen evolution reaction (HER) [18–22]. Their structure is derived from CdI_2 and $CdCl_2$ structural type and assumes a monoclinic or rhombohedral lattice configuration. For the chalcogen atom (Ch), only compounds with sulfur or selenium are known until now. Nevertheless, a vast number of metals are acknowledged to form this kind of materials, such as transition (e.g., Mn, Fe, Cd, Zn, Ni, etc.) and post-transition metals (e.g., Sn, Ga, In), as well as alkali metals like Ca and Mg [23–25]. In the past, $MPCh_3$ were deeply studied for their magnetic properties [26–28], but recent studies are mainly focused on their potential as photocatalysts for energy applications. In fact, these materials are semiconductors with band gaps between 1.3 and 3.5 eV, depending on the chalcogen elements and the metal [23,25,29].

Hydrogen production by photocatalytic water splitting represents an alternative way to the exploitation of fossil fuels, since it provides a clean source of energy that helps to solve the serious environmental problems faced by our society [30–34]. However, several factors limit

* Corresponding author at: Future Energy and Innovation Laboratory, Central European Institute of Technology, Brno University of Technology, Purkyňova 123, 61200 Brno, Czech Republic.
E-mail address: pumera.research@gmail.com (M. Pumera).

https://doi.org/10.1016/j.elecom.2021.107077
Received 15 May 2021; Received in revised form 11 June 2021; Accepted 14 June 2021
Available online 17 June 2021

the application of this technology, such as low quantum yield and low activity in the visible spectral region. 2D materials such as $MPCh_3$ have the ideal band gaps for the application as photocatalysts for hydrogen generation since they could provide more efficient use of visible light in the photocatalytic process.

In this work, we tested the photoelectrochemical performance of three different crystals metal selenophosphites ($MPSe_3$), in which M = Mn, Fe and Zn (Scheme 1). In particular, the evaluation of the ability of these materials as photoelectrocatalysts for the hydrogen evolution reaction (HER) will lead to a better understanding of their potential in solar-driven processes for clean energy production.

2. Materials and methods

2.1. Chemicals

Crystals $MPSe_3$, i.e. $MnPSe_3$, $FePSe_3$, and $ZnPSe_3$, were purchased from XFNANO, China. Screen printed carbon electrodes (SPCE, SE 101) were obtained from CH Instruments, Inc. and Indium-Tin-Oxide (ITO) coated polyethylene terephthalate (PET) from Sigma Aldrich. Conductive carbon cement EM-Tec C38 was obtained from Micro to Nano. Potassium hexacyanoferrate (III) (99%) and potassium chloride (analytical grade) were purchased from Merck. Sulfuric acid 96% was obtained from Penta, Czech Republic. All solutions were prepared in deionized water with a resistivity of 18 MΩ cm.

2.2. Materials characterization

Morphological characterization of the crystals was carried out using a scanning electron microscope (SEM) TESCAN LYRA3 with an accelerating voltage of 10 kV. The elemental analysis was obtained from energy-dispersive X-ray spectroscopy (EDS, Bruker XFlash 5010), using an accelerating voltage 20 kV. X-ray photoelectron spectroscopy (XPS) was used to evaluate the surface chemical composition. The obtained spectra were calibrated against the carbon peak C 1s (285 eV) using the CasaXPS software.

2.3. Electrochemical measurements

All electrochemical measurements were carried out using a potentiostat (PGSTAT204, Metrohm Autolab, The Netherlands) controlled by NOVA software (version 2.1), in a three-electrode configuration. A platinum wire was used as counter electrode and Ag/AgCl (1 M KCl) as reference electrode. The working electrode was varied accordingly. Cyclic voltammetry measurements were performed using $MPSe_3$ on SPCE as working electrode in 10 mM $Fe(CN)_6^{3-}$ and 0.1 M KCl electrolyte with a scan rate of 0.1 V/s.

Photocurrent measurement. Crystals of $MPSe_3$ (Figure S3) were attached to an ITO coated PET via conductive carbon tape and used as working electrodes. Chronoamperometry measurements were performed in 10 mM $Fe(CN)_6^{3-}$ and 0.1 M KCl electrolyte, applying 1 V vs. Ag/AgCl. During the experiments, the light was switched on/off at regular intervals. The illumination source was a customized LED (LZ4-40R208, LedEngin Inc.) setup that emits the wavelength 660 nm (≈40 mW/cm^2). Similar measurements were also carried out in 0.5 M H_2SO_4 electrolyte, applying −0.5 V vs. RHE. The $MPSe_3$ crystals were attached to SPCE with conductive carbon cement.

Photo-electrocatalytic hydrogen evolution measurement. The $MPSe_3$ crystals on SPCE were further used for the hydrogen evolution reaction (HER), with and without illumination. Linear sweep voltammetry (LSV) measurements were performed in 0.5 M H_2SO_4 electrolyte with a scan rate of 2 mV/s.

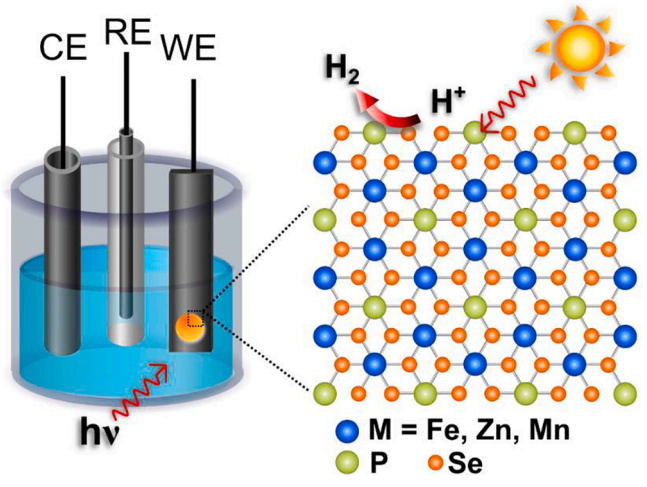

Scheme 1. Schematic illustration of the approach used to evaluate the photoelectrochemical performances of $MPCh_3$.

3. Results and discussion

The layered $MPSe_3$ materials were firstly characterized before moving to the investigation as photoelectrocatalysts for the hydrogen evolution reaction (HER). The morphology of metal selenophosphites ($MPSe_3$) crystals, namely, $MnPSe_3$, $FePSe_3$, and $ZnPSe_3$, were observed by scanning electron microscopy (SEM) (Fig. 1). All the crystals showed a structure with several stacked layers with different thicknesses, typical of the bulk 2D material. The atomic ratio between the chalcogen and the transition metal (Se/M) and the phosphorous and the metal (P/M) were calculated based on the elemental analyses using energy-dispersive X-ray spectroscopy (EDS). The EDS spectra and the distribution of the atomic % are reported in Figure S1. For all the crystals, the Se/M ratio is ~3, and the P/M ratio is ~1, which support the presence of $MPSe_3$.

The surface chemical composition of the $MPSe_3$ was further investigated using X-ray photoelectron spectroscopy (XPS). The obtained survey spectra and the key XPS peak of each element are shown in Figure S2. The presence of C 1s and O 1s peaks in all the crystals can be derivated from the adventitious carbon and oxygen as well as the carbon tape used to hold the samples for measurement. The survey spectra show that all the expected element (P, Se, and the respective metal) were detected in the analyzed crystals, confirming the observation from EDS in Figure S1.

To evaluate the electrochemical properties of the $MPSe_3$, the crystals were supported on screen printed carbon electrodes (SPCE) using conductive carbon cement. Cyclic voltammetry measurements of the $MPSe_3$ were carried out in 10 mM $Fe(CN)_6^{3-}$ and 0.1 M KCl electrolyte. The CV curves are shown in Fig. 2 and the difference between the anodic and cathodic peak potential (ΔE_p) was calculated from the voltammograms obtained. This parameter gives the information regarding the reversibility of the process: smaller ΔE_p corresponds to a more reversible electrochemical process [35]. The bare SPCE has a ΔE_p of 278 mV, and among the $MPSe_3$, $MnPSe_3$ has the lowest peak separation (149 mV), followed by $ZnPSe_3$ (154 mV) and $FePSe_3$ (252 mV).

To probe the photoelectrochemical performances, chronoamperometry experiments were carried out in the same media at the fixed potential of 1 V vs. Ag/AgCl, switching on and off the source of light (660 nm) at regular intervals. As shown in Fig. 3, the exposure to light caused an increment of the current density for all the crystals. The bare electrode does not show considerable changes in current during exposure to the light. $FePSe_3$ has the highest variation of current density after illumination, on average about 10 nA/cm^2. For $MnPSe_3$ and $ZnPSe_3$, the values are similar, approximately about 2.5 nA/cm^2. Moreover, a peak in the first seconds of illumination was observed for $ZnPSe_3$. This phenomenon is related to the recombination of the photogenerated charge carriers, that can happened for different reasons, including slow electron transport, accumulation of holes near the

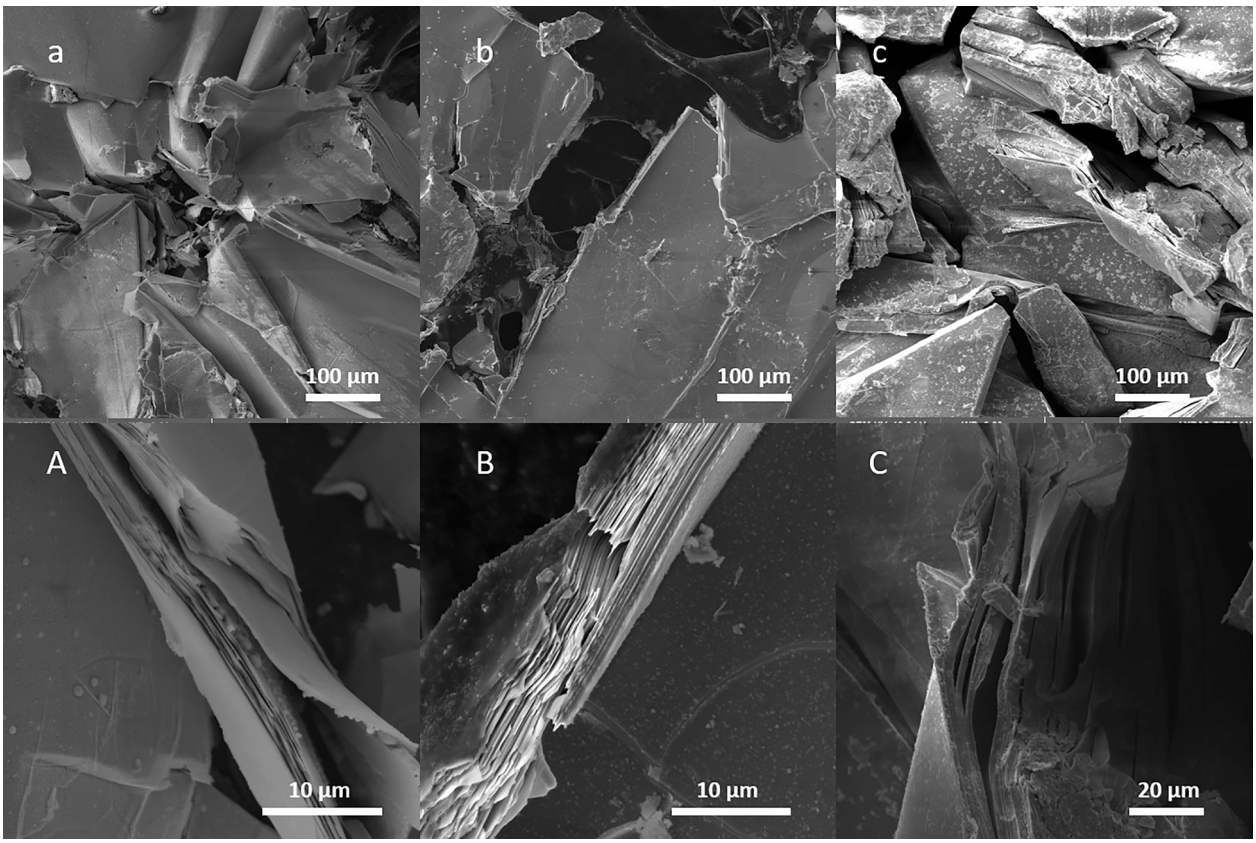

Fig. 1. SEM images of (a, A) $MnPSe_3$, (b, B) $FePSe_3$, (c, C) $ZnPSe_3$ crystals with different magnifications.

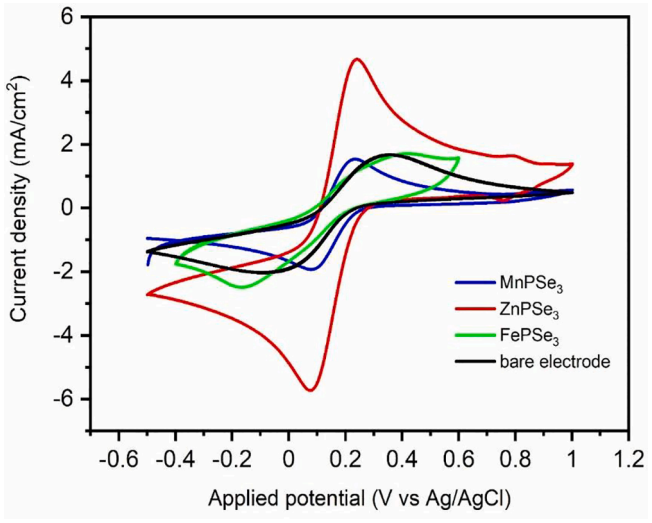

Fig. 2. Cyclic voltammograms of 10 mM $Fe(CN)_6^{3-}$ at $MPSe_3$ in 0.1 M KCl electrolyte, scan rate 0.1 V/s, screen printed carbon electrode as specimen current collector.

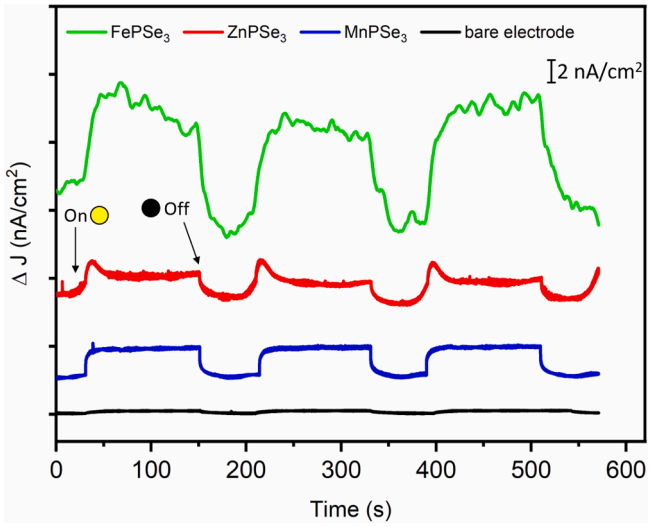

Fig. 3. Photoelectrochemical response of the $MPSe_3$ and bare electrode (as control) to visible light (660 nm) in 10 mM $Fe(CN)_6^{3-}$ and 0.1 M KCl electrolyte, applying 1 V vs. Ag/AgCl.

surface, etc. [36–38]. In general, the results obtained from the photocurrent experiment suggest that the crystals are photoactive in the visible spectral region.

Subsequently, we evaluate the photo-assisted hydrogen evolution of the three $MPSe_3$ crystals. Linear sweep voltammetry (LSV) was performed in 0.5 M H_2SO_4 with and without illumination. The overpotential at -10 mA/cm^2 has been used to compare the polarization curves obtained. The bare screen-printed carbon electrode (SPCE) is the one that shows the most deficient HER activity with an overpotential value of almost 1000 mV. The crystal trend is the same in the presence or absence of light and indicates that $ZnPSe_3$ is the material with higher catalytic activity for HER. However, all the $MPSe_3$ have a better performance with irradiation (Fig. 4A), proving the potentiality of these compounds as photocatalyst for HER. In particular, $ZnPSe_3$ is the one with the lowest overpotential (569 mV), followed by $MnPSe_3$ (655 mV) and $FePSe_3$ (740 mV). Among the three $MPSe_3$, $FePSe_3$ shows the largest improvement with illumination, with a reduced overpotential of 78 mV. $MnPSe_3$ and $ZnPSe_3$ show a decrease of the overpotential of 48 mV and

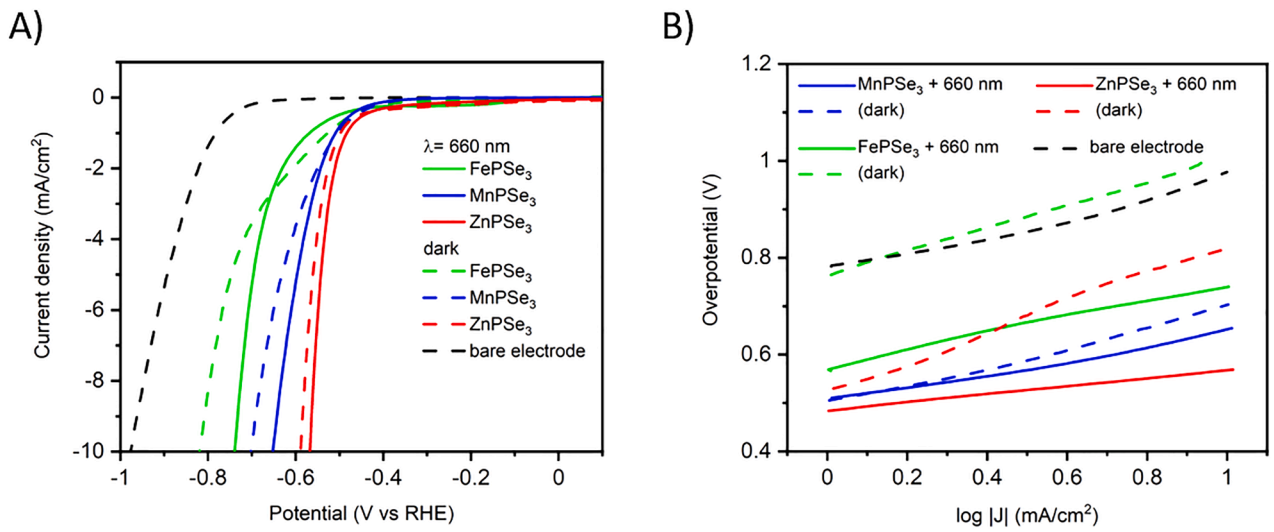

Fig. 4. Photo-electrocatalytic activity of $MPSe_3$ layered compounds evaluation for the hydrogen evolution reaction (HER). A) Linear sweep voltammograms of $MPSe_3$ and bare electrode (as control) recorded in the absence (dashed lines) and in the presence of illumination (solid lines, 660 nm) and B) corresponding Tafel plot, extrapolated from A).

44 mV respectively. These results corroborates with recent studies that report a theoretical [39] and experimental [40] band gap of ~1.5 eV for $FePSe_3$ and the consequent higher activity within the red portion of the visible spectrum. The band gaps reported for $ZnPSe_3$ and $MnPSe_3$ are 2.2–2.3 eV [40,41] and 2.2–2.9 eV [39,40], respectively, which suggest the higher activity might occur at shorter wavelength regions (<550 nm). This fact is confirmed by the absorption spectra of these compounds [40], in which the absorption of $ZnPSe_3$ and $MnPSe_3$ are confined in the range from 250 nm to 500 nm whereas $FePSe_3$ possesses an extended region up to 650 nm.

Tafel plot, represented in Fig. 4B, has been extrapolated from the LSV curves in Fig. 4A. The curves obtained by plotting the logarithm of the current density against the overpotential were used for linear fitting to obtain the Tafel slope. This value indicates the potential required to increase the current density of one order of magnitude [42]. This means that smaller overpotential and Tafel values indicate better electrocatalytic performance since less energy is required to increase the current density. In this case, the illumination catalyzes the hydrogen evolution hence decreases the Tafel slope for all the crystals. The values obtained in the presence of light are lower than the bare SPCE and, in particular, $ZnPSe_3$ is the one that shows the most significant decrease in Tafel slope value (from 315 mV/dec to 83 mV/dec), followed by $FePSe_3$ (from 240 mV/dec to 171 mV/dec) and $MnPSe_3$ (from 202 mV/dec to 143 mV/dec). The large change in the slope value observed for $ZnPSe_3$ can indicate that the rate determining step of the HER reaction is different during the exposure to the visible light. In fact, Tafel slope (b) is usually taken as an indicator of the possible reaction pathway and also to identify the limiting step of the reaction. It is known that HER in acidic media consists of two steps, adsorption and desorption. Moreover, the hydrogen desorption can proceed through two different pathways, given by Equations (1)–(3) [43,44]:

Adsorption (Volmer step):

$$H_3O^+ + e^- \rightarrow H_{ads} + H_2O;\ b \approx 118\ \text{mV/dec} \quad (1)$$

Desorption (Heyrovsky step):

$$H_{ads} + H_3O^+ + e^- \rightarrow H_2 + H_2O;\ b \approx 39\ \text{mV/dec} \quad (2)$$

Desorption (Tafel step):

$$H_{ads} + H_{ads} \rightarrow H_2;\ b \approx 29\ \text{mV/dec} \quad (3)$$

In general, for values above 118 mV/dec the determining step is the discharge reaction, or Volmer reaction, and for lower values (≈39 mV/dec for Heyrovsky reaction and ≈29.5 mV/dec for Tafel reaction) the desorption processes are the rate-determining ones [43,44].

To validate the photo-assisted catalytic effect, the photocurrent experiment was repeated in acidic media, mimicking the conditions for HER to confirm the instant photoresponse (Fig. 5). Considering the results obtained from polarization curves, we selected a potential of −0.5 V vs. RHE for chronoamperometry measurement. The results in Fig. 5 show that all the $MPSe_3$ present an instant increase in current density when exposed to the light, as well as rapid decrease when light is removed. This suggests that the photocatalytic effect is larger than the contribution from any possible convection phenomena. In particular, $FePSe_3$ and $ZnPSe_3$ show a significant change in current when exposed to light. $MnPSe_3$ is again the crystal which is less responsive to light at this particular wavelength region. Overall, the photocurrent is significantly higher compared with those obtained in a neutral media in Fig. 3. This fact can be explained considering that the measurement conducted in $Fe(CN)_6^{3-}$ involves a simple one-electron transfer reaction that is

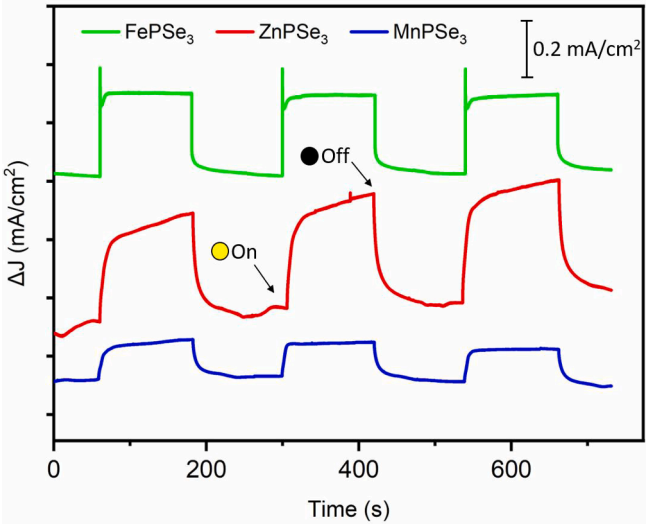

Fig. 5. Photoelectrochemical activity of layered $MPSe_3$ evaluation for the hydrogen evolution reaction. Photoresponse of the $MPSe_3$ to visible light (660 nm) in 0.5 M H_2SO_4, applying −0.5 V vs. RHE.

usually employed to evaluate the electrochemical properties of the working electrode [45]. On the other hand, the responses from the measurement in the acidic media are from a more complex reaction, as above-mentioned, in which a lot of factors can contribute to the increase in current, like the catalytic properties of the different materials toward the hydrogen generation.

4. Conclusion

In summary, we have investigated transition-metal selenophosphites crystals, $MnPSe_3$, $FePSe_3$ and $ZnPSe_3$, and we tested their performances as photoelectrocatalysts for the hydrogen evolution reaction. All the crystals showed excellent photoelectrocatalytic response during illumination with visible light (660 nm). $ZnPSe_3$ is the one that exhibited the lowest overpotential for HER and the higher response to the light during photocurrent experiments in acidic media. For this reason, among the crystals in this work, it is the most promising for the photocatalyzed production of hydrogen.

Authors contributions

M.S. performed the photoelectrochemical characterization, SEM-EDS, XPS, data analysis, and wrote the article. S.N. helped in photoelectrochemical characterization and reviewing the manuscript. M.P. came up with the idea of the project and supervised the research.

Declaration of Competing Interest

The authors declare that they have no known competing financial interests or personal relationships that could have appeared to influence the work reported in this paper.

Acknowledgment

M.P. acknowledges the financial support by the Grant Agency of the Czech Republic (GACR EXPRO: 19-26896X). M.S. acknowledges the Brno Ph.D. Talent scholarship funded by the Brno City Municipality, and the project Quality Internal Grants of BUT (KInG BUT), Reg. No. CZ.02.2.69 / 0.0 / 0.0 / 19_073 / 0016948, which is financed from the OP RDE. M.S. and S.N. thank the support of CzechNanoLab Research Infrastructure (LM2018110, MEYS CR).

Appendix A. Supplementary data

Supplementary data to this article can be found online at https://doi.org/10.1016/j.elecom.2021.107077.

References

[1] K. Maeda, T.E. Mallouk, Bull. Chem. Soc. Jpn. 92 (2018) 38–54, https://doi.org/10.1246/bcsj.20180258.
[2] I. Roger, M.A. Shipman, M.D. Symes, Nat. Rev. Chem. 1 (2017) 0003, https://doi.org/10.1038/s41570-016-0003.
[3] S. Styring, Faraday Discuss. 155 (2012) 357–376, https://doi.org/10.1039/c1fd00113b.
[4] X. Liu, S. Zhang, S. Guo, B. Cai, S.A. Yang, F. Shan, M. Pumera, H. Zheng, *Advances of 2D bismuth in energy sciences*, Chem. Soc. Rev. 49 (2020) 263–285, https://doi.org/10.1039/C9CS00551J.
[5] T.F. Jaramillo, K.P. Jørgensen, J. Bonde, J.H. Nielsen, S. Horch, I. Chorkendorff, Science 317 (2007) 100–102, https://doi.org/10.1126/science.1141483.
[6] X. Chia, M. Pumera, Chem. Soc. Rev. 47 (2018) 5602–5613, https://doi.org/10.1039/c7cs00846e.
[7] X. Chia, M. Pumera, Nat. Catal. 1 (2018) 909–921, https://doi.org/10.1038/s41929-018-0181-7.
[8] M.P. Browne, V. Urbanova, J. Plutnar, F. Novotný, M. Pumera, J. Mater. Chem. A 8 (2020) 1120–1126, https://doi.org/10.1039/c9ta11949c.
[9] W. Wang, M. Xu, X. Xu, W. Zhou, Z. Shao, Angew. Chemie - Int. Ed. 59 (2020) 136–152, https://doi.org/10.1002/anie.201900292.
[10] S. Wang, G. Liu, L. Wang, Chem. Rev. 119 (2019) 5192–5247, https://doi.org/10.1021/acs.chemrev.8b00584.
[11] N. Roy, N. Suzuki, C. Terashima, A. Fujishima, Bull. Chem. Soc. Jpn. 92 (2019) 178–192, https://doi.org/10.1246/bcsj.20180250.
[12] K.S. Novoselov, A.K. Geim, S.V. Morozov, D. Jiang, Y. Zhang, S.V. Dubonos, I. V. Grigorieva, A.A. Firsov, Science 306 (2004) 666–669, https://doi.org/10.1126/science.1102896.
[13] B. Hinnemann, P.G. Moses, J. Bonde, K.P. Jørgensen, J.H. Nielsen, S. Horch, I. Chorkendorff, J.K. Nørskov, J. Am. Chem. Soc. 127 (2005) 5308–5309, https://doi.org/10.1021/ja0504690.
[14] V. Nicolosi, M. Chhowalla, M.G. Kanatzidis, M.S. Strano, J.N. Coleman, Science 340 (2013) 72–75, https://doi.org/10.1126/science.1226419.
[15] O. Mashtalir, M.R. Lukatskaya, M.Q. Zhao, M.W. Barsoum, Y. Gogotsi, Adv. Mater. 27 (2015) 3501–3506, https://doi.org/10.1002/adma.201500604.
[16] Z. Yu, J. Peng, Y. Liu, W. Liu, H. Liu, Y. Guo, J. Mater. Chem. A 7 (2019) 13928–13934, https://doi.org/10.1039/c9ta03256h.
[17] O. Mashtalir, M. Naguib, V.N. Mochalin, Y. Dall'Agnese, M. Heon, M.W. Barsoum, Y. Gogotsi, Nat. Commun. 4 (2013) 1716, https://doi.org/10.1038/ncomms2664.
[18] C.C. Mayorga-Martinez, Z. Sofer, D. Sedmidubský, Š. Huber, A.Y.S. Eng, M. Pumera, A.C.S. Appl, ACS Appl. Mater. Interfaces 9 (2017) 12563–12573, https://doi.org/10.1021/acsami.6b16553.
[19] R. Gusmão, Z. Sofer, D. Sedmidubský, Š. Huber, M. Pumera, ACS Catal. 7 (2017) 8159–8170, https://doi.org/10.1021/acscatal.7b02134.
[20] R. Gusmão, Z. Sofer, M. Pumera, Adv. Funct. Mater. 29 (2019) 1805975, https://doi.org/10.1002/adfm.201805975.
[21] P. Sen, K. Alam, T. Das, R. Banerjee, S. Chakraborty, J. Phys. Chem. Lett. 11 (2020) 3192–3197, https://doi.org/10.1021/acs.jpclett.0c00710.
[22] D. Mukherjee, P.M. Austeria, S. Sampath, ACS Energy Lett. 1 (2016) 367–372, https://doi.org/10.1021/acsenergylett.6b00184.
[23] F. Wang, T.A. Shifa, P. Yu, P. He, Y. Liu, F. Wang, Z. Wang, X. Zhan, X. Lou, F. Xia, J. He, Adv. Funct. Mater. 28 (2018) 1802151, https://doi.org/10.1002/adfm.201802151.
[24] R. Gusmão, Z. Sofer, M. Pumera, Angew. Chemie - Int. Ed. 58 (2019) 9326–9337, https://doi.org/10.1002/anie.201810309.
[25] M.A. Susner, M. Chyasnavichyus, M.A. McGuire, P. Ganesh, P. Maksymovych, Adv. Mater. 29 (2017) 1602852, https://doi.org/10.1002/adma.201602852.
[26] D.J. Goossens, S. Brazier-Hollins, D.R. James, W.D. Hutchison, J.R. Hester, J. Magn. Magn. Mater. 334 (2013) 82–86, https://doi.org/10.1016/j.jmmm.2013.01.023.
[27] G. Long, T. Zhang, X. Cai, J. Hu, C.W. Cho, S. Xu, J. Shen, Z. Wu, T. Han, J. Lin, J. Wang, Y. Cai, R. Lortz, Z. Mao, N. Wang, ACS Nano. 11 (2017) 11330–11336, https://doi.org/10.1021/acsnano.7b05856.
[28] T. Masubuchi, H. Hoya, T. Watanabe, Y. Takahashi, S. Ban, N. Ohkubo, K. Takase, Y. Takano, J. Alloys Compd. 460 (2008) 668–674, https://doi.org/10.1016/j.jallcom.2007.06.063.
[29] R. Kumar, R.N. Jenjeti, M.P. Austeria, S. Sampath, J. Mater. Chem. C 7 (2019) 324–329, https://doi.org/10.1039/c8tc05011b.
[30] K. Maeda, K. Domen, J. Phys. Chem. Lett. 1 (2010) 2655–2661, https://doi.org/10.1021/jz1007966.
[31] A. Kudo, Y. Miseki, Chem. Soc. Rev. 38 (2009) 253–278, https://doi.org/10.1039/b800489g.
[32] J. Ran, J. Zhang, J. Yu, M. Jaroniec, S.Z. Qiao, Chem. Soc. Rev. 43 (2014) 7787–7812, https://doi.org/10.1039/c3cs60425j.
[33] K. Takanabe, ACS Catal. 7 (2017) 8006–8022, https://doi.org/10.1021/acscatal.7b02662.
[34] M. Matsuoka, M. Kitano, M. Takeuchi, K. Tsujimaru, M. Anpo, J.M. Thomas, Catal. Today. 122 (2007) 51–61, https://doi.org/10.1016/j.cattod.2007.01.042.
[35] N. Elgrishi, K.J. Rountree, B.D. McCarthy, E.S. Rountree, T.T. Eisenhart, J. L. Dempsey, J. Chem. Educ. 95 (2018) 197–206, https://doi.org/10.1021/acs.jchemed.7b00361.
[36] R. van de Krol, Photoelectrochemical measurements, in: R. van de Krol, M. Grätzel (Eds.), Photoelectrochemical Hydrogen Production, Springer, Boston, MA, 2012, pp. 69–117, https://doi.org/10.1007/978-1-4614-1380-6_3.
[37] P. Salvador, C. Gutiérrez, J. Electroanal. Chem. 160 (1984) 117–130, https://doi.org/10.1016/S0022-0728(84)80119-9.
[38] L.M. Peter, J. Li, R. Peat, J. Electroanal. Chem. 165 (1984) 29–40, https://doi.org/10.1016/S0022-0728(84)80084-4.
[39] B.L. Chittari, Y. Park, D. Lee, M. Han, A.H. Macdonald, E. Hwang, J. Jung, Phys. Rev. B 94 (2016), 184428, https://doi.org/10.1103/PhysRevB.94.184428.
[40] F.M. Oliveira, J. Paštika, L.S. Pires, Z. Sofer, R. Gusmão, Adv. Mater. Interfaces 8 (2021) 2100294, https://doi.org/10.1002/admi.202100294.
[41] J. Liu, X.B. Li, D. Wang, W.M. Lau, P. Peng, L.M. Liu, J. Chem. Phys. 140 (2014), 054707, https://doi.org/10.1063/1.4863695.
[42] C. Brett, Fundamentals of electrochemistry, in: A.A. Vives (Ed.), Piezoelectric Transducers and Applications, Springer, Berlin, Heidelberg, 2009, pp. 223–239, https://doi.org/10.1007/978-3-540-77508-9_8.
[43] M. Zeng, Y. Li, J. Mater. Chem. A 3 (2015) 14942–14962, https://doi.org/10.1039/c5ta02974k.
[44] C.G. Morales-Guio, L.A. Stern, X. Hu, Chem. Soc. Rev. 43 (2014) 6555–6569, https://doi.org/10.1039/c3cs60468c.
[45] A.J. Bard, L.R. Faulkner, Electrochemical methods: Fundamentals and Applications, 2nd ed., John Wiley & Sons Inc, New York, 2001.